Amphiphilic Dendrimers as Building Blocks in Supramolecular Assemblies

Albertus P. H. J. Schenning,[†] Cristina Elissen-Román,[†] Jan-Willem Weener,[†] Maurice W. P. L. Baars,[†] Sjerry J. van der Gaast,[‡] and E. W. Meijer*,[†]

Contribution from the Laboratory of Macromolecular and Organic Chemistry, Eindhoven University of Technology, P.O. Box 513, 5600 MB Eindhoven, The Netherlands, and the Netherlands Institute for Sea Research, P.O. Box 59, 1790 AB Den Burg, Texel, The Netherlands

Received October 23, 1997

Abstract: The self-assembly of amphiphilic dendrimers based on poly(propylene imine) dendrimers of five different generations with up to 64 end groups modified with long hydrophobic chains has been studied. At the air−water interface stable monolayers form in which the dendritic surfactants presumably adopt a cylindrical shape; all the chains are aligned perpendicular to the water surface, and the dendritic poly(propylene imine) core faces the aqueous phase. Electron microscopy and dynamic light-scattering measurements performed on aqueous solutions of the amphiphiles at pH = 1 showed the formation of small spherical aggregates with diameters varying between 20 and 200 nm. X-ray diffraction of *cast* films of these aggregates revealed bilayer thicknesses of 48−54 Å. A phase transition was detected by measuring fluorescence anisotropy. The theoretical volumes of the dendritic amphiphiles were in good agreement with those calculated from the monolayer experiments and X-ray diffraction data. Hence, the amphiphilic dendrimers within the aggregates in solution have the same highly asymmetric conformation as that proposed at the air−water interface. Calculations showed that the shape of the dendritic poly(propylene imine) core in the aggregates is distorted and that the axial ratio (r_b:r_a) ranges from 1:2.5 for the first generation to approximately 1:8 for the three highest generation of dendrimer. This behavior illustrates the high flexibility of the poly(propylene imine) dendrimers.

Introduction

The construction of supramolecular architectures having well-defined shapes and dimensions by the self-assembly of molecules is a topic of great current interest.[1−5] Dendrimers are attractive building blocks to form such materials because they are well-defined in both molecular weight and architecture.[6,7] Furthermore, as a result of their catalytic,[8] binding,[9] and optical properties,[10] supramolecular assemblies of dendrimers have potential applications in the fields of drug delivery, chemical sensors, and photosensitive materials.

Recently, we have reported on the preparation of dendritic inverted unimolecular micelles as a new class of macromolecular structures.[11] These macromolecules are based on hydrophilic poly(propylene imine) dendrimers (DAB-*dendr*-$(NH_2)_n$, where $n = 4-64$) in which all the primary amines of generations 1−5 are terminated with hydrophobic alkyl chains. These and related compounds were able to encapsulate guest molecules and could be used as very effective extractants in liquid−liquid extractions.[11−13]

As a result of their amphiphilic nature, that is, a hydrophilic poly(propylene imine) core and a hydrophobic hydrocarbon

[†] Laboratory of Macromolecular and Organic Chemistry.
[‡] Netherlands Institute for Sea Research (NIOZ).

(1) (a) Whitesides, G. M.; Mathias, J. P.; Seto, C. T. *Science* **1991**, *254*, 1312. (b) Whitesides, G. M.; Simanek, E. E.; Mathias, J. P.; Seto, C. T.; Chin, D. N.; Mammen, M.; Gordon, D. M. *Acc. Chem. Res.* **1995**, *28*, 37.

(2) Lehn, J.-M. *Angew. Chem., Int. Ed. Engl.* **1990**, *29*, 1304.

(3) Stupp, S. I.; LeBonheur, V.; Walker, K.; Li, L. S.; Huggins, K. E.; Keser, M.; Amstutz, A. *Science* **1997**, *276*, 384.

(4) (a) Zimmerman, S. C.; Zeng, F.; Reichert, D. E. C.; Kolotuchin, S. V. *Science* **1996**, *271*, 1095. (b) Huck, W. T. S.; van Veggel, F. C. J. M.; Reinhoudt, D. N. *Angew. Chem., Int. Ed. Engl.* **1996**, *35*, 1213. (c) Huck, W. T. S.; Hulst, R.; Timmerman, P.; van Veggel, F. C. J. M.; Reinhoudt, D. N. *Angew. Chem., Int. Ed. Engl.* **1997**, *36*, 1006. (d) van Hest, J. C. M.; Delnoye, D. A. P.; Baars, M. W. P. L.; van Genderen, M. H. P.; Meijer, E. W. *Science* **1995**, *268*, 1592. (e) van Hest, J. C. M.; Delnoye, D. A. P.; Baars, M. W. P. L.; Elissen-Román, C.; van Genderen, M. H. P.; Meijer, E. W. *Chem−Eur. J.* **1996**, *2*, 1616.

(5) Zeng, F.; Zimmerman, S. C. *Chem. Rev.* **1997**, *97*, 1681.

(6) (a) Tomalia, D. A. *Adv. Mater.* **1994**, *6*, 529. (b) Tomalia, D. A.; Naylor, A. M.; Goddard, W. A., III *Angew. Chem., Int. Ed. Engl.* **1990**, *29*, 138. (c) Hawker, C. J.; Frechet J. M. J. *J. Am. Chem. Soc.* **1990**, *112*, 7638. (d) Newkome, G. R.; Lin, X. *Macromolecules* **1991**, *24*, 1443. (e) Issberner, J.; Moors, R.; Vogtle, F. *Angew. Chem., Int. Ed. Engl.* **1994**, *33*, 138.

(7) (a) Newkome, G. R.; Yao, Z. Q.; Baker, G. R.; Gupta, V. K. *J. Org. Chem.* **1985**, *50*, 2003. (b) Tomalia, D. A.; Berry, V.; Hall, M.; Hestrand, D. *Macromolecules* **1987**, *20*, 1164. (c) Newkome, G. R.; Moorefield, C. N.; Baker, G. R.; Saunders, M. J.; Grossman, S. H. *Angew. Chem., Int. Ed. Engl.* **1991**, *30*, 1176. (d) Wooley, K. L.; Hawker, G. J.; Frechet, J. M. J. *J. Am. Chem. Soc.* **1993**, *115*, 11496. (e) Newkome, G. R.; Young, J. K.; Baker, G. R.; Potter, R. L.; Audoly, L.; Cooper, D.; Weiss, C. D. *Macromolecules* **1993**, *26*, 2394. (f) Hawker, C. J.; Wooley, K. L.; Frechet, J. M. J. *J. Chem. Soc., Perkin Trans. 1* **1993**, 1287.

(8) (a) Bhyrappa, P.; Young, J. K.; Moore, J. S.; Suslick, K. S. *J. Am. Chem. Soc.* **1996**, *118*, 5708. (b) Knapen, J. W. J.; van der Made, A. W.; de Wilde, J. C.; van Leeuwen, P. W. N. M.; Wijkens, P.; Grove, D. M.; van Koten, G. *Nature* **1994**, *327*, 659. (c) Reetz, M. T.; Lohmer, G.; Schwickardi, R. *Angew. Chem., Int. Ed. Engl.* **1997**, *36*, 1526. (d) Bolm, C.; Derrien, N.; Seger, A. *Synlett* **1996**, 387.

(9) Jansen, J. F. G. A.; de Brabander-van den Berg, E. M. M.; Meijer, E. W. *Science* **1994**, *226*, 1226.

(10) (a) Mekelburger, H.-B.; Rissanen, K.; Vögtle, F. *Chem. Ber.* **1993**, *126*, 1161. (b) Sadamoto, R.; Tomoka, N.; Aida, T. *J. Am. Chem. Soc.* **1996**, *118*, 3978.

(11) Stevelmans, S.; van Hest, J. C. M.; Jansen, J. F. G. A.; van Boxtel, D. A. F. J.; de Brabander-van den Berg, E. M. M.; Meijer, E. W. *J. Am. Chem. Soc.* **1996**, *118*, 7398.

(12) Baars, M. W. P. L.; Froehling, P. E.; Meijer, E. W. *Chem. Commun.* **1997**, 1959.

(13) Cooper, A. I.; Londono, J. D.; Wignall, G.; McClain, J. B.; Samulski, E. T.; Lin, J. S.; Dobrinyn, A.; Rubinstein, M.; Burke, A. L. C.; Fréchet, J. M. J.; DeSimone, J. M. *Nature* **1997**, *389*, 368.

S0002-7863(97)03677-9 CCC: $15.00
Published on Web 08/05/1998

Scheme 1

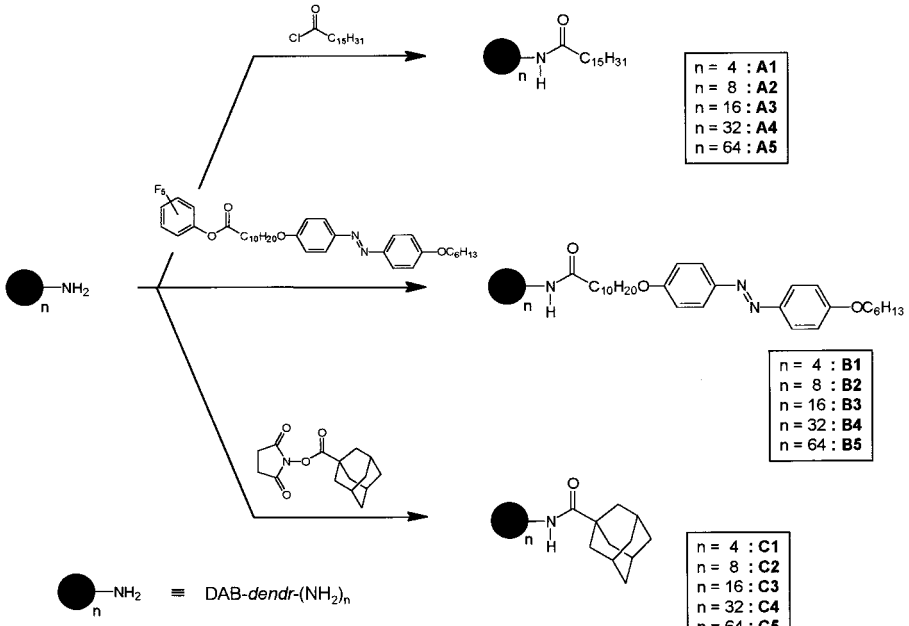

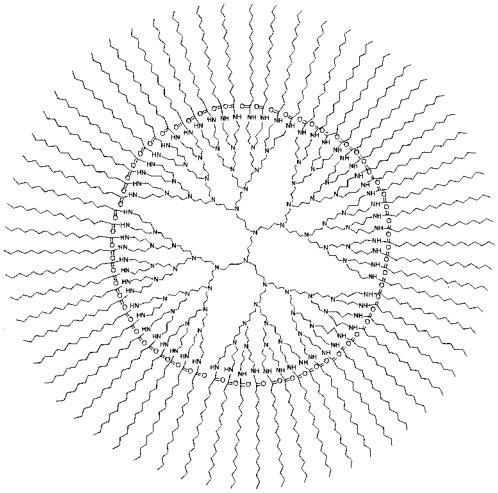

A5

shell, these types of dendrimers are suitable building blocks for the construction of supramolecular architectures in solution and at the air−water interface. In this paper, we report on the self-assembly of these amphiphilic dendrimers. It became clear during this study that these macromolecules were able to alter their conformation completely. The structure changes from a globular inverted micellar arrangement to a cylindrical amphoteric shape, in which the dendritic poly(propylene imine) part acts as a polar headgroup and the alkyl chains are packed together in parallel forming a hydrophobic unit. This observation represents an unconventional view concerning the conformational freedom of dendrimers. The high ratios found (1:8) for the radii of the dendritic part of the molecule support the findings by others of dendrimers at interfaces; however in our case the highly distorted conformation is not the result of external stimuli but of self-assembly.[14]

For the construction of supramolecular assemblies, three different kinds of functionalized dendrimers were used (Scheme 1). The first type of building blocks (**A1**−**A5**) are poly(propylene imine) dendrimers modified with palmitoyl chains at the periphery in order to obtain amphiphilic molecules.[11] In the second class of amphiphilic dendrimers (**B1**−**B5**), the alkyl chains contain an azobenzene chromophore so that information about the relative orientation of the alkyl chains with respect to each other can be monitored by UV−vis spectroscopy.[15] Finally, adamantane-modified dendrimers (**C1**−**C5**) were used as reference molecules. Bulky adamantane substituents were chosen to obtain a persistent globular conformation, similar to the *dendritic box*.[9]

(14) (a) Tomalia, D. A.; Naylor, A. M.; Goddard, W. A., III *Angew. Chem., Int. Ed. Engl.* **1990**, *29*, 138. (b) Saville, P. M.; Reynolds, P. A.; White, J. W.; Hawker, C. J.; Fréchet, J. M. J.; Wooley, K. L.; Penfold, J.; Webster, J. R. P. *J. Phys. Chem.* **1995**, *99*, 8283. (c) Tsukruk, V.; Rinderspacher, F.; Bliznyuk, V. N. *Langmuir* **1997**, *13*, 2171. (d) Tsukruk, V. *Adv. Mater.* **1998**, *10*, 253.

(15) (a) Kunitake, T.; Shimomura, M. *J. Am. Chem. Soc.* **1982**, *104*, 1757. (b) Song, X.; Perlstein, J.; Whitten, D. G. *J. Am. Chem. Soc.* **1997**, *119*, 9144.

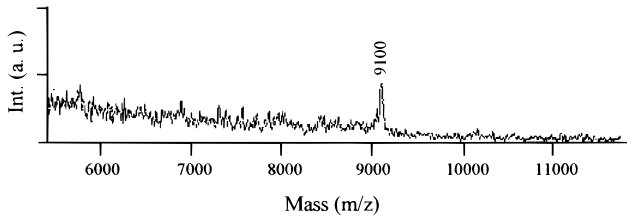

Figure 1. MALDI-TOF mass spectra of compound **B3**. $(M + K)^+ = 9100$.

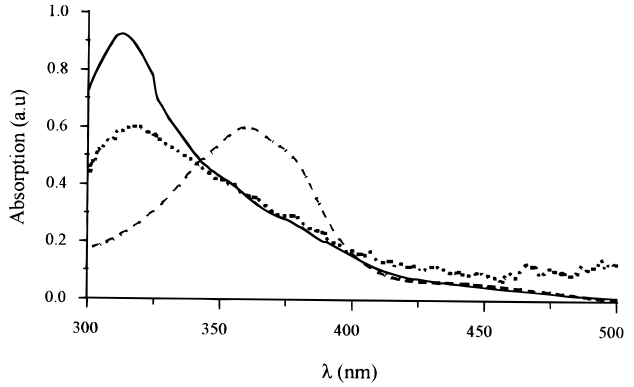

Figure 2. UV−vis spectra of compound **B4**: (- - -) CH_2Cl_2 solution; (—) aqueous solution at pH = 1; (■) monolayer on a glass substrate.

Results and Discussion

Synthesis and Characterization. Five different generations of poly(propylene imine) dendrimers, DAB-*dendr*-$(NH_2)_n$, with 4−64 primary amine end groups, were used as starting materials in the reaction with palmitoyl chloride, pentafluorphenyl 11-[4-(4-hexyloxyphenylazo)phenyloxy)] undecanoate, or 1-succinimidoyl adamantane carboxylate that yielded **A1**−**A5**, **B1**−**B5**, or **C1**−**C5**, respectively (Scheme 1).

Structural characterization of the products with ^{1}H NMR, ^{13}C NMR, and IR spectroscopy showed complete modification of the primary amines. Dendrimer generations 1−3 were further characterized with mass spectroscopy and yielded the calculated mass peaks. No defects due to incomplete reaction could be observed in the mass spectra (Figure 1). For generations 4 and 5 no mass spectra could be obtained, probably as a result of the low degree of ionization of these high-molecular-mass compounds during the MS measurements.

All dendrimers showed good solubility in apolar organic solvents. Dynamic light scattering performed on palmitoyl-modified dendrimer **A5** in dichloromethane showed single-particle behavior. Particles with a hydrodynamic diameter of 2−3 nm were observed.[16] UV measurements performed on azobenzene-modified dendrimers (**B**) in CH_2Cl_2 solutions showed the absorption of monomeric azobenzene chromophores (λ_{max} = 355 nm, Figure 2) that confirms the absence of intramolecular stacking or supramolecular aggregates in organic solution.[17]

Aggregation Behavior of Amphiphilic Dendrimers at the Air−Water Interface. The self-assembly of the different dendrimer series **A**, **B**, and **C** at the air−water interface was investigated by the Langmuir technique. The results are shown in Figure 3.

(16) (a) de Brabander, E. M. M.; Brackman, J.; Mure-Mak, M.; de Man, H.; Hogeweg, M.; Keulen, J.; Scherrenberg, R.; Coussens, B.; Mengerink, Y.; van der Wal, Sj. *Macromol. Symp.* **1996**, *102*, 9. (b) Scherrenberg, R.; Coussens, B.; van Vliet, P.; Edouard, G.; Brackman, J.; de Brabander, E. M. M.; Mortensen, K. *Macromolecules* **1998**, *31*, 456.

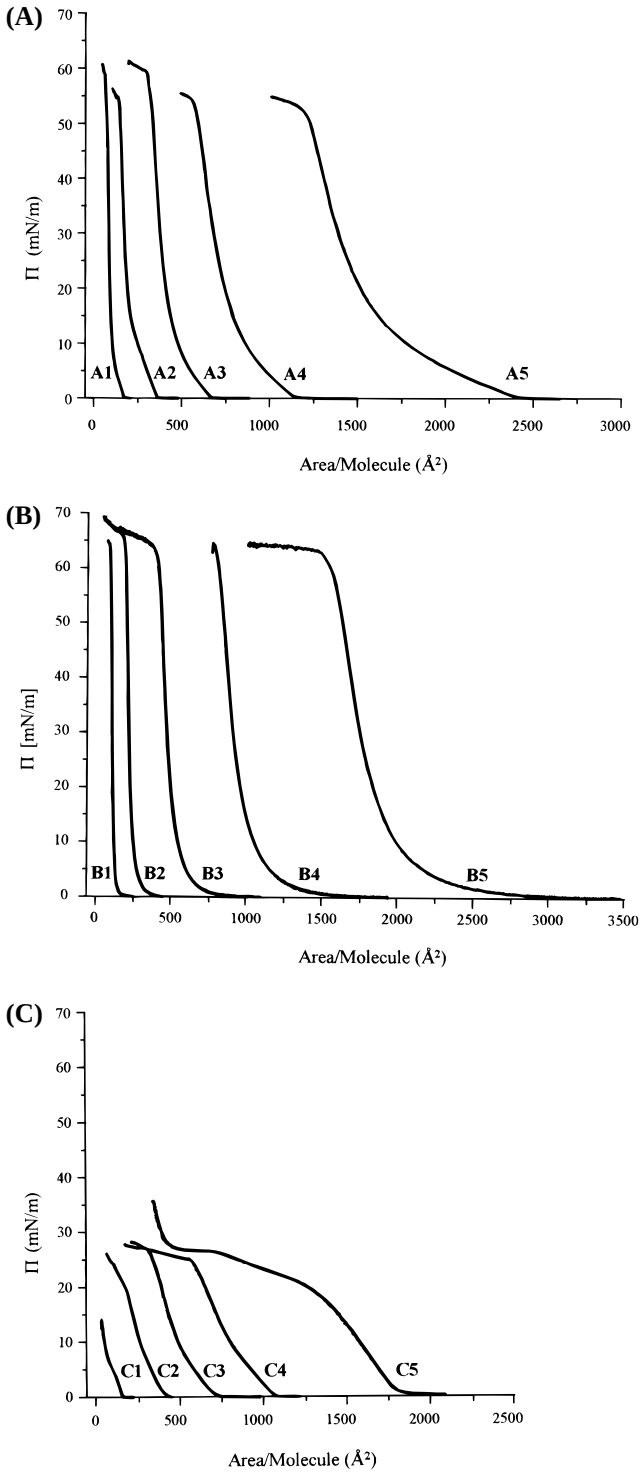

Figure 3. Compression isotherms of different generation functionalized poly(propylene imine) dendrimers at T = 25 °C, barrier speed = 50 mm^2/s; (A) isotherms of **A1**−**A5**; (B) isotherms of **B1**−**B5**; (C) isotherms of **C1**−**C5**.

The Π−*A* isotherms of adamantyl-modified dendrimers (**C**) show a behavior typical for the formation of multilayers. The isotherms of palmitoyl and azobenzene-modified dendrimers (**A** and **B**), however, display a sharp increase of the surface pressure upon compression that is indicative of the formation of stable monolayers. This stability was further supported by performing experiments at a fixed pressure (20 mN/m), in which no decrease in the area per molecule was observed during several hours. Decompression isotherms of the monolayers showed irreversibility due to the formation of aggregates on the surface of the

Table 1. Measured and Theoretical Molecular Area as a Function of the Dendrimer Generation

	A		B		C	
dendrimer generation	experimental area[a] (Å^2)	theoretical area[b] (Å^2)	experimental area[a] (Å^2)	theoretical area[c] (Å^2)	experimental area[a] (Å^2)	theoretical area[d] (Å^2)
1	107	100	124	124	160	160
2	214	200	241	248	400	320
3	442	400	521	496	700	640
4	814	800	1000	992	1070	1280
5	1600	1600	1947	1984	1800	2560

[a] Determined by extrapolation of the steep rise in surface pressure to zero pressure. [b] The area of a palmitoyl chain, in an all-trans conformation, is 25 Å^2.[21] [c] The molecular area of an alkoxy-azobenzene unit at the air/water surface was previously determined to be 31 Å^2.[19] [d] The molecular area of an adamantyl-unit is estimated to be 40 Å^2 based on CPK models.

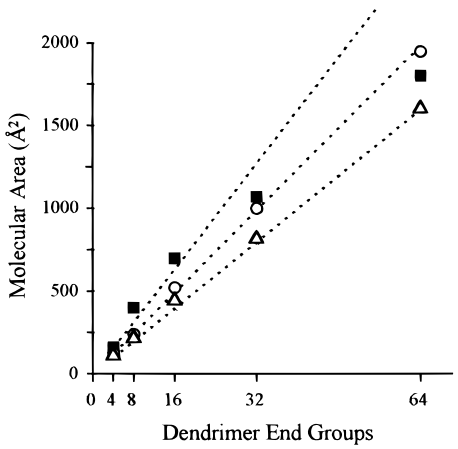

Figure 4. Molecular areas of **A1**−**A5**, **B1**−**B5**, and **C1**−**C5** as a function of dendrimer generation on the water surface: (△) **A1**−**A5**; (○) **B1**−**B5**; (■) **C1**−**C5**. Dotted lines represent theoretical values calculated by multiplying *n* (*n* = number of dendrimer end groups) by the cross-sectional area of the end groups (25 Å^2 for palmitoyl chains, 31 Å^2 for the azobenzene chains, and 40 Å^2 for adamantane units).

platinum plate when the barrier was moved backward.[18] Brewster angle microscopy (BAM) revealed the formation of preaggregates on the water surface before compression. The molecules are not uniformly distributed when they are spread out on the water surface probably due to van der Waals interactions between the aliphatic chains and $\pi-\pi$ interactions between the azobenzene moieties.[19] It was possible to transfer monolayers of the amphiphilic dendrimers to hydrophilic glass substrates. In the case of the palmitoyl-functionalized dendrimers (**A**) Z-type deposition (deposition takes place during upstroke dipping only) was observed with transfer ratios between 0.8 and 1.0 (five layers were deposited).

The area per molecule for the various dendrimers was calculated by extrapolation of the steep rise in surface pressure to zero pressure.[20] The molecular areas of **A** and **B** show a linear increase with the number of alkyl chains attached to the different generations of dendrimers (Figure 4, Table 1). If one assumes a molecular area of 25 Å^2 (a value often found for alkylcarboxylates)[21] for one palmitoyl chain and 31 Å^2 (a value found in monolayers of surfactants containing one alkyloxy-azobenzene chain)[19] for one alkyloxy-azobenzene chain, the molecular area obtained for the different generations of dendrimers corresponds precisely with 25*n* and 31*n* Å^2 (*n* = 4, 8, 16, 32, and 64) for **A** and **B**, respectively (Table 1). In contrast with the previous findings, a nonlinear dependency of the molecular area on the number of adamantane units was found for **C**. The same dependency between the number of dendrimer end groups and the molecular area determined at the air−water interface was found for the different generations of *N*-*t*-Boc-protected L-phenylalanine-modified poly(propylene imine) dendrimers (fifth generation dendrimer better known as *dendritic box*). The experimental values were roughly in agreement with the calculated ones, only in the case of **C1**−**C3**, when a molecular area of 40 Å^2 was used for one adamantane unit (based on molecular modeling simulations).

Previously, hydrophobically modified poly(amidoamine) (PAMAM) dendrimers have been studied at the air−water interface, and their behavior was described by two models.[22] For the lower-generation dendrimers, it was proposed that the hydrophilic dendrimer interior interacts with the aqueous subphase while the hydrophobically modified terminal end groups reorganize to extend outward away from the water surface. The higher-generation dendrimers were acting like hydrophobic spheroids floating at the air−water interface.

The orientation of our dendritic amphiphiles at the air−water interface can be explained by assuming one model only. All the generations presumably have an alignment in which the hydrophilic dendritic poly(propylene imine) core is pointing to the aqueous phase and all the hydrophobic tails attached to the dendritic core are oriented in a parallel fashion perpendicular to the water surface. The formation of a parallel-packed array of the alkyl chains in the monolayer was confirmed by UV−vis spectrometry. Monolayers of **B** transferred to glass substrates revealed a blue-shifted absorption maximum (λ_{max} = 316 nm, Figure 2) indicative of H-type aggregates.[23] The poly(propylene imine) core presumably has a nearly flat conformation because in that case all the attached chains count toward the observed molecular area (sketched in Figure 5), and as a consequence, a linear increase with the number of alkyl chains attached to the different generations of dendrimers is observed. In the case of **C**, this conformation of the dendritic poly(propylene imine) core is not possible due to its persistent globular structure, which results from the bulky adamantane subtituents, and no linear increase with the number of adamantane units attached to the different generations of dendrimers is observed.

Aggregation Behavior of Amphiphilic Dendrimers in Solution. When the amphiphilic dendrimers **A** and **B** were

(17) Kunitake, T.; Ihara, H.; Okahata, Y. *J. Am. Chem. Soc.* **1983**, *105*, 6070.

(18) After the Pt plate was cleaned, a curve similar to the first compression isotherm was obtained. This indicates that the progressive increase in the surface pressure, observed during decompression, is due to the formation of aggregates on the metal surface.

(19) Maack, J.; Ahuja, R. C.; Tachibana, H. *J. Phys. Chem.* **1995**, *99*, 9221.

(20) Saville, P. A.; Reynolds, P. A.; White, J. W.; Hawker, C. J.; Fréchet, J. M. J.; Wooley, K. L.; Penfold, J.; Webster, J. R. P. *J. Phys. Chem.* **1995**, *99*, 8283.

(21) (a) Small, D. M. *The Physical Chemistry of Lipids*; Plenum Press: New York, 1986. (b) Fendler, J. H. *Membrane Mimetic Chemistry*; Wiley: New York, 1982.

(22) Sayed-Sweet, Y.; Hedstrand, D. M.; Spinder, R.; Tomalia, D. A. *J. Mater. Chem.* **1997**, *7*, 199.

(23) Shimomura, M.; Kunitake, T. *Chem. Lett.* **1981**, 1001.

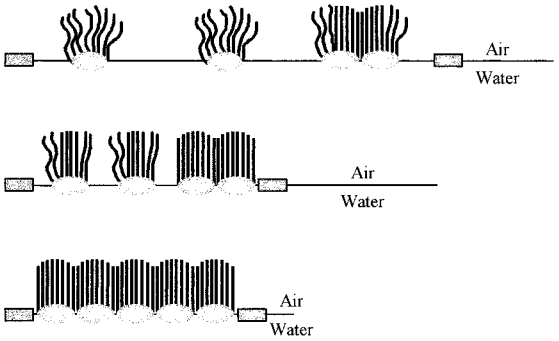

Figure 5. Schematic representation of the organization of amphiphilic dendrimers in a monolayer on the water surface.

Table 2. Experimental Data for the Different Generations of Palmitoyl-Modified Dendrimers (**A1**−**A5**)

dendrimer generation	size vesicles EM (nm)[a]	CAC (M)	bilayer thickness (Å)[b]
A1		1.0×10^{-6}	51
A2	35−140	6.2×10^{-7}	51 (41)
A3	35−200	6.3×10^{-7}	48 (42)
A4	35−130	6.3×10^{-7}	57 (50)
A5	20−140	2.2×10^{-7}	54

[a] Solutions of **A1** and **A2** were measured immediately after preparation due to their instability. The size of aggregates of **A1** could not be estimated due to the high degree of cluster formation. [b] The values in parentheses are additional periodicities corresponding to lower intensity signals in the X-ray diffraction patterns.

dispersed in buffered water (pH = 1), opalescent solutions were obtained. Dispersions of the first- and second-generation dendritic amphiphiles precipitated within 1 day, whereas the higher- generation aggregates were stable for several weeks as was judged by measuring the time-dependent change in turbidity at 450 nm.[24] Adamantyl-modified dendrimers could not be dispersed in water at all, even at very low pH, presumably due to the persistent, rigid, hydrophobic shell around the dendritic core.

Several techniques were used to obtain information about the molecular organization of aggregates of **A** and **B** and will be discussed in the following section.

(a) Transmission Electron Microscopy (TEM). Three different visualization techniques have been used to investigate the aggregation behavior of **A** and **B** in acidic aqueous solutions. Pictures obtained with the Pt-shadowing technique displayed the presence of spherical aggregates with diameters of 20−140 nm (Table 2, Figure 6). The formation of clusters was commonly observed. When uranyl acetate was used as a negative staining agent, comparable results were obtained. The formation of clusters is probably due to the two visualization techniques used, which involve draining and evaporating water. It is well-known that cryoelectron microscopy is a more reliable technique to observe individual aggregates in solution.[25] Cryo-TEM confirmed the presence of globular aggregates in solution (Figure 6). The particle size observed was about 60−130 nm, which is in the same order of magnitude as that found with the previous two techniques. In the case of aggregates formed by **A**, striations could be observed with a thickness of ca. 5 nm. This thickness is comparable with the distances found by X-ray

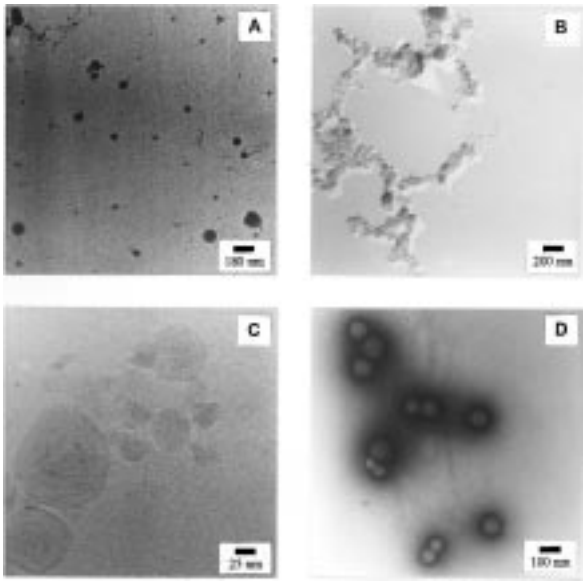

Figure 6. Transmission electron microscopy: (A) cryoelectron picture of a 10^{-5} M dispersion of **B5** in a 0.1 N HCl water solution; (B) picture of a 10^{-5} M dispersion of **B5** in a 0.1 N HCl water solution. (sample shaded with Pt); (C) cryoelectron photograph of a 5×10^{-5} M dispersion of **A5** in a 0.1 N HCl water solution; (D) TEM picture of a 1×10^{-4} M dispersion of **A5** in a glycine/hydrochloride buffer solution (pH = 1) (sample stained with uranyl acetate).

diffraction experiments carried out on *cast* films of acidic aqueous dispersions of **A** and presumably corresponds to bilayer aggregates (vide infra).

(b) Dynamic Light Scattering. The particle size distributions of aggregate solutions of **A** and **B** were also determined with dynamic light scattering (DLS). The average particle diameter values for both palmitoyl- and azobenzene-modified dendrimers of generations 3−5 was 55 nm (data not shown) with a relatively broad distribution (average width of 40 nm). Moreover, no large aggregates (>150 nm) were found. These results are in good agreement with the results obtain by TEM. DLS measurements exhibited the presence of clusters in solution at rather high concentrations ($>10^{-5}$ M), which could be significantly minimized upon dilution.

(c) Critical Aggregation Concentration. The critical aggregation concentrations (CAC) of palmitoyl modified dendrimers (**A**) were determined using pyrene as probe molecule[26] and are shown in Table 2. No significant differences were found between the CAC's for different generations, and the values were all very low (10^{-6}−10^{-7} M), as expected for amphiphilic polymers.[26]

(d) Fluorescence Depolarization. Changes in the microviscosity of bilayers can be investigated by the fluorescence depolarization technique.[27] For this purpose, all-*trans*-1,6-diphenyl-1,3,5-hexatriene (DPH) was used as a fluorescence polarization probe in acidic aqueous solutions of **A3**−**A5** (because of the instability of aggregates of **A1** and **A2**, no accurate measurements could be performed on these solutions). A high anisotropy value (r = 0.31) was found at room temperature, reflecting a high microviscosity in the bilayer (Figure 7). At that temperature the alkyl chains are below their phase-transition temperature and behave as stiff chains. When

(24) Chong, C. S.; Colbow, K. *Biochim. Biophys. Acta* **1976**, *436*, 260.
(25) (a) Frederik, P. M.; Stuart, M. C. A.; Bomans, P. H. H.; Lasic, D. D. In *Handbook of Nonmedical Applications of Liposomes*; Lasic, D. D., Barenholz, Y., Eds.; CRC Press: Boca Raton, FL, 1996; p 309. (b) Kilpatrick, P. K.; Miller, W. G.; Talmon, Y. In *Surfactants in Solution*, Mittal, K. L., Bothorel, P., Eds.; Plenum: New York, 1986; Vol. 4, p 489.
(26) (a) Wang, L. Y.; Winnik, M. A. *Langmuir* **1990**, *6*, 1437. (b) Wilhem, M.; Zhao, C.; Wang, L. Y.; Xu, R.; Winnik, M. A. *Macromolecules* **1991**, *24*, 1033. (c) Yekta, A.; Duhamel, J.; Brochard, P.; Adiwidjaja, H.; Winnik, M. A. *Macromolecules* **1993**, *26*, 1829. (d) Kalyasundaram, K.; Thomas, J. K. *J. Am. Chem. Soc.* **1977**, *99*, 2039. (e) Astafieva, I.; Zhong, X. F.; Eisenberg, A. *Macromolecules* **1993**, *26*, 7339.

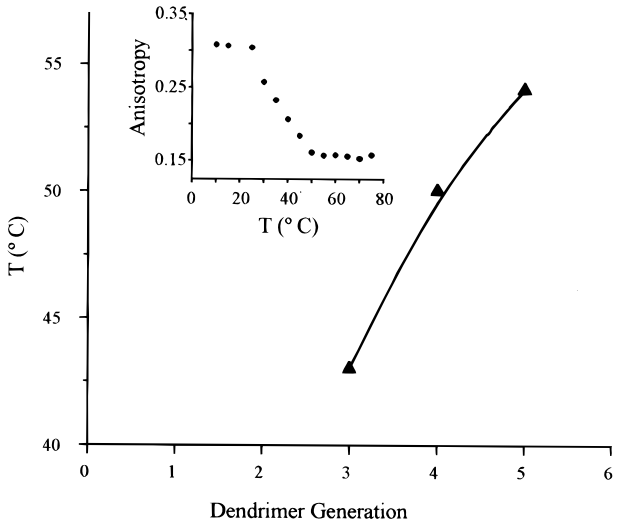

Figure 7. Phase-transition temperature of the aggregates formed by **A3**−**A5** in acidic water. Inset: temperature profile of fluorescence anisotropy measured on a solution of **A4** labeled with DPH.

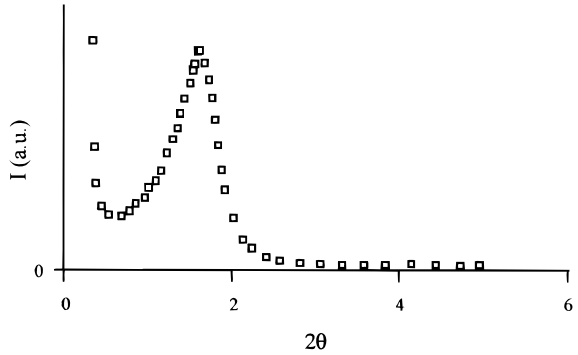

Figure 8. X-ray diffraction curve of *cast* films of **A5**.

the temperature increased, the anisotropy dropped from 0.31 to 0.15 at a certain point corresponding to the gel-to-liquid-crystalline phase-transition temperature (T_t). The T_t increases upon going to a higher generation, that is, increasing of the number of alkyl chains that are covalently bonded to the headgroup of the molecule (Figure 8). This observation suggests that the packing of the alkyl chains becomes better when going to higher generations.[27] Moreover, the presence of a sharp transition temperature (T_t) indicates that the amphiphilic molecules are arranged in a well-organized cooperative form.

(e) X-ray Diffraction (XRD). X-ray diffraction was carried out on *cast* films of acidic aqueous dispersions of **A** dried on a silicon plate in vacuo (Figure 8). The diffraction patterns displayed clear periodicities between 48 and 54 Å for the different generations, with additional periodicities in some cases (Table 2). These distances correspond very well with the striations of 5 nm observed by cryo-TEM (vide supra).

Since the extended molecular length of a palmitoyl chain as estimated from Corey−Pauling−Koltun (CPK) models is approximately 22 Å, the observed thickness can correspond to that of a bilayer in which the dendrimers possess a nonspherical shape. The additional periodicities in the diffraction patterns can be a result of small domains in which the bilayers are tilted or interdigitated.

(f) Osmotic Behavior. Osmotic experiments were performed to investigate if the spherical aggregates contain an inner

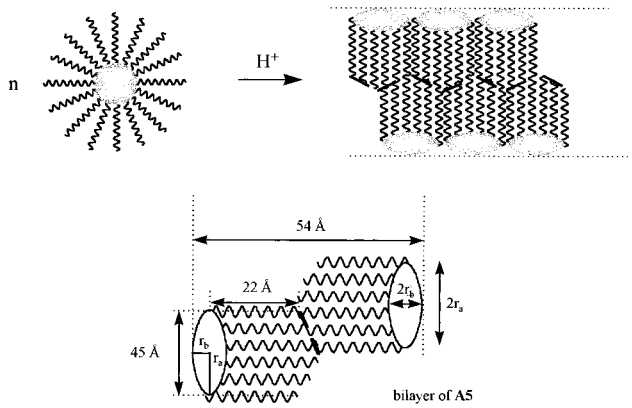

Figure 9. Top: schematic representation of bilayer formation of amphiphilic dendrimers. Bottom: degree of flattening of the poly(propylene imine) part of **A**5. The major radius (Table 3), r_a, was calculated from the molecular area (Table 1) found by monolayer experiments (in the case of **A5**: 1600 Å^2 = πr_a^2, r_a = 22.6 Å). The length of palmitoyl chains based on molecular modeling is 22 Å. The thickness of the bilayer of **A5** (Table 2), measured by XRD, is 54 Å. This value corresponds to 2 times the length of the palmitoyl chain plus 3 times r_b ($2 \times 22 + 3r_b = 54$ Å, assuming that the two layers of amphiphilic dendrimers are positioned as illustrated), yielding a minor radius of r_b = 3.3 Å for **A5**.

aqueous compartment. If such a water compartment is present and the aggregate is permeable to water but impermeable to a solute, it should display osmotic swelling and shrinkage.[28] In a typical experiment, aggregates of **A5** containing 0.5 M sucrose were added to 0.03−0.80 M sucrose solutions. The absorbance at 450 nm, which is related to the volume of the aggregate, was measured as a function of sucrose concentration in the outer aqueous phase.[28] A decrease in absorption was found when the external sucrose concentration was increased. This result indicates that aggregates of **A5** behave as osmometers and therefore must contain an inner water compartment.

On the basis of the presented data on the aggregates in solution, we suggest the same conformation of the amphiphilic dendrimers in the spherical aggregates in solution as that proposed for the monolayers obtained with the Langmuir technique. The hydrophilic, protonated, dendritic part faces the aqueous phase while the aliphatic chains are packed parallel forming an apolar layer. Upon dispersion of the amphiphilic dendrimers in acidic water, the poly(propylene imine) unit becomes protonated, which leads to a more extended conformation of the dendritic core as a result of Coulombic repulsion.[29,30] An extended conformation could facilitate the changes in shape of the dendrimer; at the moment that the dendritic interior goes outside, the hydrophobic chains tumble and are coming together forming parallel-packed bilayers (Figure 9). The presence of such a bilayer is supported by UV−vis measurements (Figure 2) performed on aggregate solutions of **B** that showed a λ_{max} at 316 nm, which is indicative of H-type aggregates of the azobenzene units.[23] Assuming that the globular structures (electron microscopy) are composed of bilayers and have an inner compartment of water (osmotic experiments), we propose

(27) (a) Shinitzky, M.; Barenholz, Y. *Biochim. Biophys. Acta* **1978**, *515*, 367. (b) Lentz, B. R. *Chem. Phys. Lipids* **1993**, *64*, 99. (c) Borenstain, V.; Barenholz, Y. *Chem. Phys. Lipids* **1993**, *64*, 117.

(28) (a) Bangham, A. D.; De Gier, J.; Greville, G. D. *Chem. Phys. Lipids* **1967**, *1*, 225. (b) Kano, K.; Romero, A.; Djermouni, B.; Ache, H. J.; Fendler, J. H. *J. Am. Chem. Soc.* **1979**, *101*, 4030.

(29) Young, J. K.; Baker, G. R.; Newkome, G. R.; Morris, K. F.; Johnson, S., Jr. *Macromolecules* **1994**, *27*, 3464.

(30) A pK_a value of 6.5 for the tertiary amines of the poly(propylene imine) dendrimers was determined; see Koper, G. J. M.; van Genderen, M. H. P.; Elissen-Román, C.; Baars, M. W. P. L.; Meijer, E. W.; Borkovec, M. *J. Am. Chem. Soc.* **1997**, *119*, 6512.

Table 3. Molecular Volumes of the Different Generations of Dendrimer (**A1**−**A5**)

dendrimer generation	calcd hydrod. radius (Å)[a]	calcd molecular volume (Å^3)[b]	measd molecular volume (Å^3)[c]	major radius r_a (Å)[d]	minor radius r_b (Å)[e]	axial ratio r_a:r_b
A1	6.3	3000	2730	5.8	2.3	2.5:1
A2	7.7	5820	5460	8.3	2.3	3.6:1
A3	9.5	11400	10600	11.9	1.3	9:1
A4	12.9	24500	20350	16.1	2.0	8:1
A5	16.1	48580	43200	22.6	3.3	7:1

[a] Dendrimer hydrodynamic radius obtained with molecular simulations in the gas phase and SANS measurements.[16] [b] Theoretical volume of dendritic amphiphiles was calculated by taking the sum of the volume of palmitoyl chains (one chain based on CPK models = 484 Å^3) and the volume of the dendrimer part (based on dendrimer hydrodynamic radius). [c] Obtained by multiplying half of bilayer thickness (X-ray measurements, Table 2) by the molecular area (monolayer experiments, Table 1). [d] r_a was calculated from the molecular area by considering the transversal section of the dendrimer part to be a circle. [e] r_b was calculated by making the approximation that the alkyl chains are in an all-trans conformation.

that these amphiphilic dendrimers are self-assembled into vesicles.

The Dendritic Structure. If we assume a cylindrical shape of the amphiphilic dendrimers at the air−water interface and in acidic aqueous solution, we can compare the theoretical molecular volumes with those obtained from experimental techniques (Table 3).[31] The van der Waals volume of the palmitoyl chains has been estimated at 484 Å^3 per chain based on CPK models. The calculated hydrodynamic radius of the DAB-*dendr*-$(NH_2)_n$ part has been obtained from small-angle neutron scattering measurements as well as from molecular simulations in the gas phase.[14,32] The theoretical volume of the whole molecule was obtained by taking the sum of the volume of all the palmitoyl chains attached to the core and the volume of the poly(propylene imine) part. The experimental volume of the amphiphilic dendrimers was calculated by multiplying half of the bilayer thickness from the XRD data by the molecular area derived from monolayer experiments.[31] The calculated volumes of the amphiphilic dendrimers agree with the theoretical volumes and support the assumption that the conformation of the amphiphilic dendrimers is cylindrical in both acidic aqueous solution and at the air−water interface.

It is well-known that dendrimers can flatten and spread out on surfaces.[13,33] The degree of flattening of the dendritic poly(propylene imine) part in the supramolecular assemblies can be calculated from the experimental data by assuming that it has the shape of an oblate spheroid, where r_a is the major radius and r_b the minor radius (Figure 9). The calculated values for r_a and r_b are given in Table 3. The calculations showed that the shape of the dendrimer is distorted and that the axial ratio (r_b:r_a) ranges from 1:2.5 for the first generation to approximately 1:8 for the three highest generations of dendrimers.

Conclusions

Dendritic amphiphiles based on poly(propylene imine) dendrimers modified with long hydrophobic chains represent a novel class of surfactants and introduce new perspectives toward functional materials. Langmuir experiments at the air−water interface demonstrated that these molecules are able to arrange themselves in monolayers in which the dendrimer part of the molecule is in contact with the water subphase and the alkyl chains are all pointing toward the air, forming a parallel-packed hydrophobic layer. In potential, the deposition of these monolayers on a solid substrate makes it possible to construct materials with nonlinear properties based on dendrimers functionalized with optical units.[14,34] It was not feasible to obtain a well-defined monolayer in the case of dendrimers containing adamantane groups because they were too bulky to allow the dendrimer to effectively change its conformation.

When the amphiphilic dendrimers were dissolved in acidic water, the formation of small spherical aggregates was observed. Presumably, the poly(propylene imine) unit becomes protonated, which leads to a more extended conformation; the dendritic interior goes outside and the hydrophobic chains tumble, coming together to form well-packed layers in which all the alkyl chains are oriented parallel to each other. The amphiphilic dendrimers within the aggregates presumably have the same cylindrical conformation as that proposed at the air−water interface. Calculations showed that the shape of the dendrimer is distorted and that the axial ratio (r_b:r_a) ranges from 1:2.5 for the first generation to approximately 1:8 for the three highest generations of dendrimers.

The photoswitching properties of aggregates of azobenzene-funtionalized dendrimers (**B1**−**B5**) are of interest in the fields of controlled release and optical data storage and are currently under investigation.

Experimental Section

General Methods. UV spectra were recorded on a Perkin-Elmer UV−vis−NIR Lambda 900 spectrometer. A Branson 2210 sonication bath was used for the preparation of dispersions in acidic water. Steady-state fluorescence spectra were run in a Perkin-Elmer luminescence spectrometer LS 50B in the right-angle geometry (90° collecting optics) using slit openings of 5 nm for emission and 2.5 nm for excitation. Dynamic light-scattering experiments were performed in a Malvern autosizer instrument, with a 5 mW laser (633 nm), and the samples were filtrated with 1 μm polysulfonate filters to eliminate dust particles in solution before the measurement was taken. Low-angle X-ray powder diffraction measurements were performed with a self-made instrument (Netherlands Institute for Sea Research, NIOZ, Texel). This high-accuracy $\theta-\theta$ diffractometer is equipped with a Cu tube, variable divergence and antiscatter slits, and an energy dispersive Si/Li Kevex detector, which enables a high peak-to-background ratio.

Materials. THF (Biosolve, p.a.) was distilled over Na/K/benzophenone under an argon atmosphere. Diethyl ether (p.a.) was used without further purification. Triethylamine (Fluka, p.a.) was stored on KOH pellets. Palmitoyl chloride (Aldrich, 98%), 1-adamantanecarboxylic acid (Acros, 99%), *N*-hydroxysuccinimide (Acros, 98+%), 1,3-dicylcohexylcarbodiimide (DCC) (Aldrich, 99%), 4-hexyloxyaniline (Aldrich, 99%), phenol (Merck, p.a.), sodium nitrite (Merck, 99%), 11-bromoundecanoic acid (Acros, 99+%), pentafluorophenol (Aldrich, 99+%), D(+)-sucrose (Janssen 99+%), pyrene (Aldrich, 98%), and DPH (Aldrich, 98%) were used as received.

(31) For bilayer-forming surfactants it is believed that the cross section of the headgroup is roughly the same as that of the hydrophobic part of the amphiphile; see Israelachvelli, J. N.; Mitchell, D. J.; Ninham, B. W. *J. Chem. Soc., Faraday Trans. 2* **1976**, *72*, 1525.

(32) It should be mentioned that the radius of the dendrimers in the gas phase will be different from that in solution. Also, protonation will change the radius of the dendrimers. Molecular modeling shows a hydrodynamic radius of 20.5 Å for the *protonated* fifth generation dendrimer, while for the *unprotonated* one a radius of 16.1 Å was calculated.

(33) Mansfield, M. L. *Polymer* **1996**, *37*, 3835.

(34) (a) Ou, S. H.; Percec, V.; Mann, J. A.; Lando, J. B.; Zhou, L.; Suger, K. D. *Macromolecules* **1993**, *26*, 7263. (b) Ou, S. H.; Percec, V.; Mann, J. A.; Lando, J. B. *Langmuir* **1994**, *10*, 905.

1-Succinimidoyl adamantane carboxylate was synthesized according to standard peptide coupling techniques using DCC as the coupling reagent.[35] Pentafluorphenyl 11-[4-(4-hexyloxyphenylazo)phenyl-oxy)] undecanoate is synthesized by a method analogous to a literature procedure,[17] which uses DCC as a coupling reagent to obtain the activated ester and will be published in more detail elsewhere.

Typical Procedure for Palmitoyl-Functionalized Dendrimers (A3). Triethylamine (41.8 g, 0.41 mol) was added to a solution of DAB-*dendr*-$(NH_2)_{16}$ (6.23 g, 3.69 mmol) in THF (300 mL). Palmitoyl chloride (22.8 g, 0.083 mol) was slowly added over a period of 10 min. After being stirred for 43 h, the turbid solution was evaporated in vacuo. The residue was refluxed with a NaOH solution (1 M, 300 mL) for 2.5 h. The solution was precipitated and washed with a NaOH solution (1 M, 300 mL) and subsequently with demineralized water, yielding the crude product. The product was refluxed in diethyl ether and centrifugated to remove salts. After the solution was decanted, the residue was mixed with diethyl ether and centrifugated again. The combined organic layers were evaporated in vacuo, yielding **A3** (15.0 g, 74%) as a yellowish product. Mp 77 °C. ^{1}H NMR (400 MHz, $CDCl_3$): δ = 0.88 (t, 48H, C*H*$_3$), 1.18−1.75 (m, 476H, CH$_3$(C*H*$_2$)$_{13}$ + NCH$_2$C*H*$_2$C*H*$_2$CH$_2$N + NCH$_2$C*H*$_2$CH$_2$N + NCH$_2$C*H*$_2$CH$_2$NHCO), 2.16 (t, 32H, C*H*$_2$CONH), 2.31−2.45 (m, 84H, NC*H*$_2$CH$_2$CH$_2$C*H*$_2$N + NC*H*$_2$CH$_2$C*H*$_2$N + C*H*$_2$CH$_2$CH$_2$NHCO), 3.25 (q, 32H, C*H*$_2$NHCO), 7.26 (t, 16H, N*H*CO). ^{13}C NMR (100 MHz, $CDCl_3$): δ = 14.1 (*C*H$_3$), 22.7 (CH$_3$*C*H$_2$), 24.9 (NCH$_2$*C*H$_2$*C*H$_2$CH$_2$N + NCH$_2$*C*H$_2$CH$_2$N), 26.0 (*C*H$_2$CH$_2$CONH), 27.1 (*C*H$_2$CH$_2$NHCO), 29.3−29.7 (CH$_3$CH$_2$CH$_2$(*C*H$_2$)$_{10}$), 31.9 (CH$_3$CH$_2$*C*H$_2$), 36.7 (*C*H$_2$CONH), 37.8 (*C*H$_2$NHCO), 51.4 (*C*H$_2$CH$_2$CH$_2$NHCO), 52.2 (NC*H*$_2$CH$_2$C*H*$_2$N), 54.5 (NC*H*$_2$CH$_2$CH$_2$*C*H$_2$N), 173.8 (NH*C*O). IR (KBr): ν (cm^{-1}) = 3299.0 (N−H stretch), 2918.1 (C−H sat.), 1639.9 (C═O), 1560.0 (N−H bend). Anal. Calcd for $C_{344}H_{688}N_{30}O_{16}$: C, 75.10; H, 12.60; N, 7.64. Found: C, 74.86; H, 12.59; N, 7.72. FAB-MS: calcd for $C_{344}H_{688}N_{30}O_{16}$ 5501.49; found 5500.1.

A1. Mp 115 °C. ^{1}H NMR ($CDCl_3$): δ = 0.88 (t, 12H, C*H*$_3$), 1.18−1.62 (m, 116H, CH$_3$(C*H*$_2$)$_{13}$ + NCH$_2$C*H*$_2$C*H*$_2$CH$_2$N + NCH$_2$C*H*$_2$CH$_2$CH$_2$NHCO), 2.15 (t, 8H, C*H*$_2$CONH), 2.31−2.45 (m, 12H, NC*H*$_2$CH$_2$CH$_2$C*H*$_2$N + C*H*$_2$CH$_2$CH$_2$NHCO), 3.28 (q, 8H, C*H*$_2$NHCO), 6.51 (t, 4H, N*H*CO). ^{13}C NMR ($CDCl_3$): δ = 14.1 (*C*H$_3$), 22.7 (CH$_3$*C*H$_2$), 25.1 (NCH$_2$*C*H$_2$*C*H$_2$CH$_2$N), 25.9 (*C*H$_2$CH$_2$CONH), 27.1 (*C*H$_2$CH$_2$NHCO), 29.5−29.7 (CH$_3$CH$_2$CH$_2$(*C*H$_2$)$_{10}$), 31.9 (CH$_3$CH$_2$*C*H$_2$), 36.9 (*C*H$_2$CONH), 38.2 (*C*H$_2$NHCO), 52.0 (*C*H$_2$CH$_2$CH$_2$NHCO), 53.9 (NC*H*$_2$CH$_2$CH$_2$*C*H$_2$N), 173.4 (NH*C*O). IR (KBr): ν (cm^{-1}) = 3319.2 (N−H stretch), 2918.2 (C−H sat.), 1638.4 (C═O), 1549.1 (N−H bend). Anal. Calcd for $C_{80}H_{160}N_6O_4$: C, 75.65; H, 12.70; N, 6.62. Found: C, 75.79; H, 12.77; N, 6.59. FAB-MS: calcd for $C_{344}H_{688}N_{30}O_{16}$ 1270.2; found 1270.0 (M + H)$^+$.

A2. Mp 75 °C. ^{1}H NMR (400 MHz, $CDCl_3$): δ = 0.90 (t, 24H, C*H*$_3$), 1.18−1.75 (m, 236H, CH$_3$(C*H*$_2$)$_{13}$ + NCH$_2$C*H*$_2$C*H*$_2$CH$_2$N + NCH$_2$C*H*$_2$CH$_2$N + C*H*$_2$CH$_2$NHCO), 2.17 (t, 16H, C*H*$_2$CONH), 2.31−2.45 (m, 36H, NC*H*$_2$CH$_2$CH$_2$C*H*$_2$N + NC*H*$_2$CH$_2$C*H*$_2$N + C*H*$_2$CH$_2$CH$_2$NHCO), 3.28 (q, 16H, C*H*$_2$NHCO), 6.95 (t, 8H, N*H*CO). ^{13}C NMR (100 MHz, $CDCl_3$): δ = 14.1 (*C*H$_3$), 22.7 (CH$_3$*C*H$_2$), 24.9 (NCH$_2$*C*H$_2$CH$_2$CH$_2$N + NCH$_2$*C*H$_2$CH$_2$N), 26.0 (*C*H$_2$CH$_2$CONH), 27.1 (*C*H$_2$CH$_2$NHCO), 29.4−29.7 (CH$_3$CH$_2$CH$_2$(*C*H$_2$)$_{10}$), 31.9 (CH$_3$CH$_2$*C*H$_2$), 36.8 (*C*H$_2$CONH), 37.9 (*C*H$_2$NHCO), 51.6 (NC*H*$_2$CH$_2$CH$_2$NHCO), 52.2 (NC*H*$_2$CH$_2$C*H*$_2$N), 54.5 (NC*H*$_2$CH$_2$CH$_2$*C*H$_2$N), 173.6 (NH*C*O). IR (KBr): ν (cm^{-1}) = 3319.2 (N−H stretch), 2918.2 (C−H sat.), 1638.4 (C═O), 1549.1 (N−H bend). Anal. Calcd for $C_{168}H_{336}N_{14}O_8$: C, 75.65; H, 12.70; N, 6.62. Found: C, 75.79; H, 12.77; N, 6.59. FAB-MS: calcd for $C_{168}H_{336}N_{14}O_8$ 2680.61; found 2680.59 (M + H)$^+$.

A4. Mp 78 °C. ^{1}H NMR (400 MHz, $CDCl_3$): δ = 0.88 (t, 96H, C*H*$_3$), 1.20−1.70 (m, 956H, CH$_3$(C*H*$_2$)$_{13}$ + NCH$_2$C*H*$_2$C*H*$_2$CH$_2$N + NCH$_2$C*H*$_2$CH$_2$N + C*H*$_2$CH$_2$NHCO), 2.16 (t, 64H, C*H*$_2$CONH), 2.31−2.45 (m, 180H, NC*H*$_2$CH$_2$CH$_2$C*H*$_2$N + NC*H*$_2$CH$_2$C*H*$_2$N + C*H*$_2$CH$_2$CH$_2$NHCO), 3.25 (q, 64H, C*H*$_2$NHCO), 7.42 (t, 32H, N*H*CO). ^{13}C NMR (100 MHz, $CDCl_3$): δ = 14.1 (*C*H$_3$), 22.7 (CH$_3$*C*H$_2$), 26.0 (*C*H$_2$CH$_2$CONH), 27.1 (*C*H$_2$CH$_2$NHCO), 29.4−29.8 (CH$_3$CH$_2$CH$_2$(*C*H$_2$)$_{10}$), 31.9 (CH$_3$CH$_2$*C*H$_2$), 36.6 (*C*H$_2$CONH), 37.7 (*C*H$_2$NHCO), 51.4 (*C*H$_2$CH$_2$CH$_2$NHCO), 52.3 (NC*H*$_2$CH$_2$C*H*$_2$N), 173.9 (NH*C*O). IR (KBr): ν (cm^{-1}) = 3300.4 (N−H stretch), 2918.0 (C−H sat.), 1637.0 (C═O), 1560.0 (N−H bend). Anal. Calcd for $C_{696}H_{1392}N_{62}O_{32}$ (11 143.05): C, 75.02; H, 12.59; N, 7.79. Found: C, 74.91; H, 12.28; N, 7.76.

A5. Mp 77 °C. ^{1}H NMR (400 MHz, $CDCl_3$): δ = 0.89 (t, 192H, C*H*$_3$), 1.20−1.75 (m, 1916H, CH$_3$(C*H*$_2$)$_{13}$ + NCH$_2$C*H*$_2$C*H*$_2$CH$_2$N + NCH$_2$C*H*$_2$CH$_2$N + C*H*$_2$CH$_2$NHCO), 2.19 (br t, 128H, C*H*$_2$CONH), 2.31−2.45 (m, 372H, NC*H*$_2$CH$_2$CH$_2$C*H*$_2$N + NC*H*$_2$CH$_2$C*H*$_2$N + C*H*$_2$CH$_2$CH$_2$NHCO), 3.25 (br t, 128H, C*H*$_2$NHCO), 7.64 (s, 64H, N*H*CO). ^{13}C NMR (100 MHz, $CDCl_3$): δ = 14.1 (*C*H$_3$), 22.7 (CH$_3$*C*H$_2$), 26.1 (*C*H$_2$CH$_2$CONH), 27.2 (*C*H$_2$CH$_2$NHCO), 29.4−29.8 (CH$_3$CH$_2$CH$_2$(*C*H$_2$)$_{10}$), 31.9 (CH$_3$CH$_2$*C*H$_2$), 36.6 (*C*H$_2$CONH), 37.6 (*C*H$_2$NHCO), 51.3 (*C*H$_2$CH$_2$CH$_2$NHCO), 52.2 (NC*H*$_2$CH$_2$C*H*$_2$N), 174.0 (NH*C*O). IR (KBr): ν (cm^{-1}) = 3299.8 (N−H stretch), 2917.0 (C−H sat.), 1640.6 (C═O), 1552.2 (N−H bend). Anal. Calcd for $C_{1400}H_{2800}N_{126}O_{64}$ (22 426.34): C, 74.98; H, 12.58; N, 7.87. Found: C, 74.51; H, 12.57; N, 7.83.

Typical Procedure for 11-[4-(4-Hexyloxyphenylazo)phenyloxy]-undecanoyl-Functionalized Dendrimers (B3). DAB-*dendr*-$(NH_2)_{16}$ (186 mg, 0.11 mmol) was dissolved in DMF (10 mL). To this solution was slowly added a solution of pentafluorphenyl 11-[4-(4-hexyloxyphenylazo)phenyl-oxy)] undecanoate (1.256 g, 1.94 mmol) in DMF (20 mL) in a dropwise fashion. After this addition was complete, the reaction mixture was refluxed for 2 h yielding a homogeneous, red solution. The product precipitated upon cooling to room temperature. Filtration and subsequent washing with diethyl ether yielded **B3** (0.83 g, 83%) as a yellow powder. Mp 138 °C. ^{1}H NMR (300 MHz, $CDCl_3$): δ = 0.92 (t, 48H, C*H*$_3$), 1.20−1.85 (m, 380H, CH$_3$(C*H*$_2$)$_4$ + (C*H*$_2$)$_8$CH$_2$CONH + C*H*$_2$CH$_2$NHCO + NCH$_2$C*H*$_2$CH$_2$N + NCH$_2$C*H*$_2$C*H*$_2$CH$_2$N), 2.18 (t, 32H, C*H*$_2$CONH), 2.40 (m, 84H, NC*H*$_2$CH$_2$CH$_2$C*H*$_2$N + NC*H*$_2$CH$_2$C*H*$_2$N + C*H*$_2$CH$_2$CH$_2$NHCO), 3.27 (q, 32H, C*H*$_2$NHCO), 4.00 (m, 64H, C*H*$_2$O), 6.87 (t, 16H, N*H*CO), 6.96 (d, 64H, C*H*$_{ortho}$), 7.84 (d, 64H, C*H*$_{meta}$). ^{13}C NMR (75 MHz, $CDCl_3$): δ = 14.4 (*C*H$_3$), 23.0 (CH$_3$*C*H$_2$), 26.2−32.1 (NCH$_2$*C*H$_2$*C*H$_2$CH$_2$N + NCH$_2$*C*H$_2$CH$_2$N + CH$_3$CH$_2$(*C*H$_2$)$_3$ + (*C*H$_2$)$_8$CH$_2$CONH + *C*H$_2$CH$_2$NHCO), 37.2 (*C*H$_2$CONH), 38.4 (*C*H$_2$NHCO), 52.3 (*C*H$_2$CH$_2$CH$_2$NHCO), 53.0 (NC*H*$_2$CH$_2$C*H*$_2$N + NC*H*$_2$CH$_2$CH$_2$C*H*$_2$N), 69.0 (*C*H$_2$O), 115.3 (*C*H$_{ortho}$), 124.8 (*C*H$_{meta}$), 147.7 (*C*−N═N−*C*), 161.8 (O*C*$_{phenyl}$), 174.0 (NH*C*O). UV−vis (CH_2Cl_2): λ_{max} = 355 nm. IR (KBr): ν (cm^{-1}) = 3285 (N−H stretch), 3071 (sec. N−H stretch), 2926 (C−H sat.), 1641 (C═O), 1552 (N−H bend). MALDI-TOF-MS: calcd for $C_{552}H_{784}N_{62}O_{48}$ 9056.7; found 9100 (M + K)$^+$.

B1. Mp 161 °C. ^{1}H NMR (300 MHz, $CDCl_3$): δ = 0.93 (t, 12H, C*H*$_3$), 1.20−1.52 (m, 76H, CH$_3$(C*H*$_2$)$_3$ + (C*H*$_2$)$_6$CH$_2$CH$_2$CONH + NCH$_2$C*H*$_2$C*H*$_2$CH$_2$N), 1.62 (m, 16H, C*H*$_2$CH$_2$NHCO + C*H*$_2$CH$_2$CONH), 1.81 (m, 16H, C*H*$_2$CH$_2$O), 2.16 (t, 8H, C*H*$_2$CONH), 2.42 (m, 12H, NC*H*$_2$CH$_2$CH$_2$C*H*$_2$N + C*H*$_2$CH$_2$CH$_2$NHCO), 3.29 (q, 8H, C*H*$_2$NHCO), 4.03 (m, 16H, C*H*$_2$O), 6.29 (t, 4H, N*H*CO), 6.95 (d, 16H, C*H*$_{ortho}$), 7.82 (d, 16H, C*H*$_{meta}$). ^{13}C NMR (75 MHz, $CDCl_3$): δ = 14.4 (*C*H$_3$), 23.0 (CH$_3$*C*H$_2$), 25.7 (NCH$_2$*C*H$_2$*C*H$_2$CH$_2$N), 26.2−32.1 (CH$_3$CH$_2$(*C*H$_2$)$_3$ + (*C*H$_2$)$_8$CH$_2$CONH + *C*H$_2$CH$_2$NHCO), 37.3 (*C*H$_2$CONH), 38.7 (*C*H$_2$NHCO), 52.7 (*C*H$_2$CH$_2$CH$_2$NHCO), 54.6 (NC*H*$_2$CH$_2$CH$_2$C*H*$_2$N), 69.0 (*C*H$_2$O), 115.3 (*C*H$_{ortho}$), 124.8 (*C*H$_{meta}$), 147.7 (*C*−N═N−*C*), 161.8 (O*C*$_{phenyl}$), 173.7 (NH*C*O). UV−vis (CH_2Cl_2): λ_{max} = 355 nm. IR (KBr): ν (cm^{-1}) = 3281 (N−H stretch), 3073 (sec. N−H stretch), 2925 (C−H sat.), 1641 (C═O), 1554 (N−H bend). MALDI-TOF-MS: calcd for $C_{132}H_{200}N_{14}O_{12}$ 2175.13; found 2197 (M + Na)$^+$, 2213 (M + K)$^+$. ESI-MS: found 2176 (M + H)$^+$, 1088 (M + 2H)$^{2+}$, 726 (M + 3H)$^{3+}$, 545 (M + 4H)$^{4+}$.

B2. Mp 136 °C. ^{1}H NMR (300 MHz, $CDCl_3$): δ = 0.93 (t, 24H, C*H*$_3$), 1.20−1.85 (m, 220H, CH$_3$(C*H*$_2$)$_4$ + (C*H*$_2$)$_8$CH$_2$CONH + C*H*$_2$CH$_2$NHCO + NCH$_2$C*H*$_2$CH$_2$N + NCH$_2$C*H*$_2$C*H*$_2$CH$_2$N), 2.17 (t, 16H, C*H*$_2$CONH), 2.41 (m, 36H, NC*H*$_2$CH$_2$CH$_2$C*H*$_2$N + NC*H*$_2$CH$_2$C*H*$_2$N + C*H*$_2$CH$_2$CH$_2$NHCO), 3.28 (q, 16H, C*H*$_2$NHCO), 4.02 (m, 32H, C*H*$_2$O), 6.64 (t, 8H, N*H*CO), 6.97 (d, 32H, C*H*$_{ortho}$), 7.84 (d, 32H, C*H*$_{meta}$). ^{13}C NMR (75 MHz, $CDCl_3$): δ = 13.9 (*C*H$_3$), 22.5 (CH$_3$*C*H$_2$), 24.9 (NCH$_2$*C*H$_2$CH$_2$N), 25.7−31.6 (NCH$_2$*C*H$_2$*C*H$_2$CH$_2$N + CH$_3$CH$_2$(*C*H$_2$)$_3$ + (*C*H$_2$)$_8$CH$_2$CONH + *C*H$_2$CH$_2$NHCO), 36.7 (*C*H$_2$CONH), 37.9 (*C*H$_2$NHCO), 51.9 (*C*H$_2$CH$_2$CH$_2$NHCO), 52.2 (NC*H*$_2$CH$_2$C*H*$_2$N + NC*H*$_2$CH$_2$CH$_2$C*H*$_2$N), 68.5 (*C*H$_2$O), 114.8 (*C*H$_{ortho}$), 124.3 (*C*H$_{meta}$), 147.3 (*C*−N═N−*C*), 161.3 (O*C*$_{phenyl}$), 173.6 (NHCO). UV−vis (CH$_2$-

(35) Anderson, G. W.; Zimmerman, J. E.; Callahan, F. M. *J. Am. Chem. Soc.* **1964**, *86*, 1839.

Cl_2): λ_{max} = 355 nm. IR (KBr): ν (cm^{-1}) = 3286 (N−H stretch), 3071 (sec. N−H stretch), 2926 (C−H sat.), 1641 (C═O), 1553 (N−H bend). MALDI-TOF-MS: calcd for $C_{272}H_{416}N_{30}O_{24}$ 4490.49; found 4514 $(M + Na)^+$, 4530 $(M + K)^+$. ESI-MS: found (after deconvolution) 4490 $(M)^+$.

B4. Mp 140 °C. ^{1}H NMR (300 MHz, $CDCl_3$): δ = 0.92 (t, 96H, C*H*$_3$), 1.20−1.85 (m, 892H, $CH_3(CH_2)_4$ + $(CH_2)_8CH_2CONH$ + CH_2-CH_2NHCO + $NCH_2CH_2CH_2N$ + $NCH_2CH_2CH_2CH_2N$), 2.18 (t, 64H, C*H*$_2$CONH), 2.40 (m, 180H, $NCH_2CH_2CH_2CH_2N$ + $NCH_2CH_2CH_2N$ + $CH_2CH_2CH_2NHCO$), 3.26 (m, 64H, C*H*$_2$NHCO), 3.99 (m, 128H, C*H*$_2$O), 7.12 (t, 32H, N*H*CO), 6.95 (d, 128H, C*H*$_{ortho}$), 7.83 (d, 128H, C*H*$_{meta}$). ^{13}C NMR (75 MHz, $CDCl_3$): δ = 13.9 (*C*H$_3$), 22.6 (CH_3CH_2), 25.7−31.6 ($NCH_2CH_2CH_2CH_2N$ + $NCH_2CH_2CH_2N$ + $CH_3CH_2(CH_2)_3$ + $(CH_2)_8CH_2CONH$ + CH_2CH_2NHCO), 36.7 (*C*H$_2$CONH), 37.9 (CH_2-NHCO), 51.8 ($CH_2CH_2CH_2NHCO$), 52.4 ($NCH_2CH_2CH_2N$ + NCH_2-$CH_2CH_2CH_2N$), 68.5 (*C*H$_2$O), 114.9 (*C*H$_{ortho}$), 124.3 (*C*H$_{meta}$), 147.3 (*C*−N═N−*C*), 161.3 (O*C*$_{phenyl}$), 173.7 (NH*C*O). UV−vis (CH_2Cl_2): λ_{max} = 355 nm. IR (KBr): ν (cm^{-1}) = 3289 (N−H stretch), 3071 (sec. N−H stretch), 2926 (C−H sat.), 1640 (C═O), 1554 (N−H bend).

B5. Mp 134 °C. ^{1}H NMR (300 MHz, $CDCl_3$): δ = 0.92 (t, 192H, C*H*$_3$), 1.20−1.90 (m, 1788H, $CH_3(CH_2)_4$ + $(CH_2)_8CH_2CONH$ + CH_2-CH_2NHCO + $NCH_2CH_2CH_2N$ + $NCH_2CH_2CH_2CH_2N$), 2.17 (t, 128H, C*H*$_2$CONH), 2.41 (m, 372H, $NCH_2CH_2CH_2CH_2N$ + $NCH_2CH_2CH_2N$ + $CH_2CH_2CH_2NHCO$), 3.27 (m, 128H, C*H*$_2$NHCO), 4.02 (m, 256H, C*H*$_2$O), 7.25 (t, 64H, N*H*CO), 6.98 (d, 256H, C*H*$_{ortho}$), 7.85 (d, 256H, C*H*$_{meta}$). ^{13}C NMR (75 MHz, $CDCl_3$): δ = 13.9 (*C*H$_3$), 22.6 (CH_3 CH_2), 25.7−33.3 ($NCH_2CH_2CH_2CH_2N$ + $NCH_2CH_2CH_2N$ + CH_3-$CH_2(CH_2)_3$ + $(CH_2)_8CH_2CONH$ + CH_2CH_2NHCO), 36.8 (*C*H$_2$CONH), 38.0 (*C*H$_2$NHCO), 51.8 ($CH_2CH_2CH_2NHCO$), 52.4 ($NCH_2CH_2CH_2N$ + $NCH_2CH_2CH_2CH_2N$), 68.6 (*C*H$_2$O), 114.9 (*C*H$_{ortho}$), 124.3 (*C*H$_{meta}$), 147.3 (*C*−N═N−*C*), 161.4 (O*C*$_{phenyl}$), 173.3 (NH*C*O). UV−vis (CH_2-Cl_2): λ_{max} = 355 nm. IR (KBr): ν (cm^{-1}) = 3290 (N−H stretch), 3073 (sec. N−H stretch), 2926 (C−H sat.), 1640 (C═O), 1552 (N−H bend).

Typical Procedure for Adamantyl-Functionalized Dendrimers (C3). To a solution of DAB-*dendr*-$(NH_2)_{16}$ (200 mg, 0.12 mmol) in CH_2Cl_2 (15 mL) was added 1-succinimidoyl adamantane carboxylate (653 mg, 2.372 mmol). The reaction mixture was stirred for 24 h, and subsequently an equal volume of a NaOH solution (1 M) was added. After 16 h, the organic phase was extracted and the solvent was evaporated in vacuo to yield the crude product. The product was taken up in a CH_2Cl_2/MeOH mixture (99:1 v/v) and filtered over silica to remove residual salts, yielding **C3** (350 mg, 69%) as a white foam. Mp 119 °C. ^{1}H NMR (400 MHz, $CDCl_3$): δ = 1.38 (s, 4H, $NCH_2CH_2CH_2CH_2N$), 1.54 (m, 24H, $NCH_2CH_2CH_2N$), 1.62 (q, 32H, CH_2CH_2NHCO), 1.67−1.76 (m, 96H, *H*-4), 1.85 (s, 96H, CH_2, *H*-2), 2.03 (s, 48H, *H*-3), 2.38−2.43 (m, 84H, $NCH_2CH_2CH_2CH_2N$ + NCH_2-CH_2CH_2N + $CH_2CH_2CH_2NHCO$), 3.29 (q, 32H, CH_2NHCO), 6.67 (t, 16H, N*H*CO). ^{13}C NMR (100 MHz, $CDCl_3$): δ = 24.7 (NCH_2CH_2-CH_2N), 25.1 ($NCH_2CH_2CH_2CH_2N$), 26.8 (CH_2CH_2NHCO), 28.2 (*C*-3), 36.6 (*C*-4), 38.3 (CH_2NHCO), 39.4 (*C*-2), 40.5 (*C*-1), 52.0 ($CH_2CH_2CH_2NHCO$), 52.1−52.6 ($NCH_2CH_2CH_2N$), 54.4 (NCH_2CH_2-CH_2CH_2N), 178.1 (NH*C*O). IR (KBr): ν (cm^{-1}) = 3299.0 (N−H stretch), 2903.6 (C−H sat.), 1636.4 (C═O), 1527.6 (N−H bend). FAB-MS: calcd for $C_{264}H_{432}N_{30}O_{16}$ 4285.5; found 4281.8.

C1. Mp 117 °C. ^{1}H NMR (400 MHz, $CDCl_3$): δ = 1.41 (s, 4H, $NCH_2CH_2CH_2CH_2N$), 1.61 (q, 8H, CH_2CH_2NHCO), 1.67−1.76 (m, 24H, *H*-4), 1.85 (s, 24H, *H*-2), 2.03 (s, 12H, *H*-3), 2.38 (s, 4H, NCH_2-$CH_2CH_2CH_2N$), 2.43 (t, 8H, $CH_2CH_2CH_2NHCO$), 3.29 (dt, 8H, CH_2-NHCO), 6.40 (t, 4H, N*H*CO). ^{13}C NMR (100 MHz, $CDCl_3$): δ = 24.9 ($NCH_2CH_2CH_2CH_2N$), 26.8 ($NCH_2CH_2CH_2N$), 28.1 (*C*-3), 36.6 (*C*-4), 38.3 (CH_2NHCO), 39.3 (*C*-2), 40.5 (*C*-1), 52.0 ($CH_2CH_2CH_2$-NHCO), 54.1 ($NCH_2CH_2CH_2CH_2N$), 178.0 (NH*C*O). IR (KBr): ν (cm^{-1}) = 3354.4 cm^{-1} (N−H stretch), 2904.0 (C−H sat.), 1636.4 (C═O), 1527.8 (N−H bend). FAB-MS: calcd for $C_{60}H_{96}N_6O_4$ 965.46; found 965.44 $(M + H)^+$.

C2. Mp 118 °C. ^{1}H NMR (400 MHz, $CDCl_3$): δ = 1.36 (s, 4H, $NCH_2CH_2CH_2CH_2N$), 1.54 (m, 8H, $NCH_2CH_2CH_2N$), 1.61 (q, 16H, CH_2CH_2NHCO), 1.67−1.76 (m, 48H, *H*-4), 1.85 (s, 48H, *H*-2), 2.03 (s, 24H, *H*-3), 2.37 (m, 20H, $NCH_2CH_2CH_2CH_2N$ + $NCH_2CH_2CH_2N$), 2.42 (t, 16H, $CH_2CH_2CH_2NHCO$), 3.29 (q, 16H, CH_2NHCO), 6.56 (t, 8H, N*H*CO). ^{13}C NMR (400 MHz, $CDCl_3$): δ = 24.7 (NCH_2CH_2-CH_2N), 25.1 ($NCH_2CH_2CH_2CH_2N$), 26.8 (CH_2CH_2NHCO), 28.2 (*C*-3), 36.6 (*C*-4), 38.3 (CH_2NHCO), 39.4 (*C*-2), 40.5 (*C*-1), 52.1 ($CH_2CH_2CH_2NHCO$), 52.6 ($NCH_2CH_2CH_2N$), 54.2 ($NCH_2CH_2CH_2$-CH_2N), 178.1 (NH*C*O). IR (KBr): ν (cm^{-1}) = 3355.9 (N−H stretch), 2903.6 (C−H sat.), 1636.4 (C═O), 1522.3 (N−H bend). FAB-MS: calcd for $C_{128}H_{208}N_{14}O_8$ 2071.1; found 2071.87 $(M + H)^+$.

C4. Mp 119 °C. ^{1}H NMR (400 MHz, $CDCl_3$): δ = 1.38 (s, 4H, $NCH_2CH_2CH_2CH_2N$), 1.50−1.65 (m, 120H, $NCH_2CH_2CH_2N$ + CH_2-CH_2NHCO), 1.67−1.75 (m, 192H, *H*-4), 1.86 (s, 192H, *H*-2), 2.02 (s, 96H, *H*-3), 2.38−2.43 (m, 180H, $NCH_2CH_2CH_2CH_2N$ + NCH_2-CH_2CH_2N + $CH_2CH_2CH_2NHCO$), 3.29 (q, 64H, CH_2NHCO), 6.81 (t, 32H, N*H*CO). ^{13}C NMR (100 MHz, $CDCl_3$): δ = 24.3 (NCH_2CH_2-CH_2N), 24.5 ($NCH_2CH_2CH_2N$), 24.9 ($NCH_2CH_2CH_2CH_2N$), 26.8 (CH_2-CH_2NHCO), 28.1 (*C*-3), 36.6 (*C*-4), 38.1 (CH_2NHCO), 39.4 (*C*-2), 40.5 (*C*-1), 51.9 ($CH_2CH_2CH_2NHCO$), 52.0−52.5 ($NCH_2CH_2CH_2N$), 54.4 ($NCH_2CH_2CH_2CH_2N$), 178.0 (NH*C*O). IR (KBr): ν (cm^{-1}) = 3357.9 (N−H stretch), 2904.0 (C−H sat.), 1636.0 (C═O), 1528.0 (N−H bend).

C5. Mp 120 °C. ^{1}H NMR (400 MHz, $CDCl_3$): δ 1.38 (s, 4H, $NCH_2CH_2CH_2CH_2N$), 1.50−1.65 (m, 248H, $NCH_2CH_2CH_2N$ + CH_2-CH_2NHCO), 1.66−1.75 (m, 384H, *H*-4), 1.86 (s, 384H, *H*-2), 2.02 (s, 192H, *H*-3), 2.30−2.55 (m, 372H, $NCH_2CH_2CH_2CH_2N$ + NCH_2-CH_2CH_2N + $CH_2CH_2CH_2NHCO$), 3.28 (br, 128H, CH_2NHCO), 6.95 (t, 64H, N*H*CO). ^{13}C NMR (100 MHz, $CDCl_3$): δ = 24.4 (NCH_2CH_2-CH_2N), 24.7 ($NCH_2CH_2CH_2N$), 25.0 ($NCH_2CH_2CH_2CH_2N$), 26.9 (CH_2-CH_2NHCO), 28.2 (*C*-3), 36.6 (*C*-4), 38.2 (CH_2NHCO), 39.3 (*C*-2), 40.5 (*C*-1), 51.9 ($CH_2CH_2CH_2NHCO$), 52.0−52.5 ($NCH_2CH_2CH_2N$), 54.4 ($NCH_2CH_2CH_2CH_2N$), 178.1 (NH*C*O). IR (KBr): ν (cm^{-1}) = 3354.4 (N−H stretch), 2904.0 (C−H sat.), 1636.4 (C═O), 1527.8 (N−H bend).

Preparation of Aqueous Solutions. The desired amount of dendrimer was dissolved in 100 μL of methanol/THF (1:2 v/v). The resulting solution was injected into 10 mL of a buffer solution of pH = 1 (preheated at 60 °C) with stirring. The aqueous solution was placed in a bath-type sonicator and sonicated for 10 min at room temperature.

Electron Microscopy. Samples for transmission electron microscopy were prepared by the negative-staining and Pt-shading methods. A droplet of acidic aqueous solution was placed on a Cu grid, covered with Formvar, and allowed to dry for 1 min, after which the droplet was removed with filter paper. Negative staining was performed by addition of a droplet of a 1 wt % uranyl acetate solution over 1 min. Pt-shaded samples were prepared by covering the dried sample with Pt using a Balzers sputter unit (Pt layer thickness = 2 nm). These samples were studied using a Philips TEM 201 (60 kV) (University of Nijmegen). For cryoelectron microscopy, thin films were prepared by dipping a 700-mesh copper grid in the suspension and blotting it with filter paper to remove the excess liquid. The thin films that formed between the bars of the grid were vitrified by plunging them into melting ethane. The vitrified films were stored under liquid nitrogen and observed at −170 °C with a Philips CM12 microscope at low-dose conditions, 120 kV (University of Maastricht). In the case of palmitoyl-modified dendrimers (**A**), the material was very sensitive to the electron beam, while in the case of azobenzene-containing dendrimers (**B**), the stability of the sample was better.

Fluorescence Measurements. A 1 cm square quartz cell was filled with ca. 3 mL of solution, with [pyrene] = 4.8×10^{-7} M. In the case of fluorescence emission spectra λ_{ex} = 339 nm, and for excitation spectra λ_{em} = 390 nm. All samples were prepared by adding a known amount of pyrene in acetone to a series of empty 10 mL volumetric flasks; after evaporation of the acetone, known amounts of a stock solution of polymer were added and diluted with a buffer of pH = 1 to obtain final dendrimer concentrations between 10^{-4} and 10^{-9} M. The flasks were sealed, protected from light, and stirred for ca. 20 h at room temperature to allow the pyrene and the aggregates to equilibrate. For the fluorescence anisotropy measurements, DPH was dissolved together with the polymer in an aqueous buffer pH = 1 by the ethanol injection method. The ratio of alkyl chains attached to the poly(propylene imine) part to probe was 25:1. For fluorescence emission spectra λ_{ex} = 382 nm, and for the excitation spectra λ_{em} = 430 nm. The sample was thermostated by using a thermocouple in the sample holder connected to a RTE 110 Neslab thermostated, ethyleneglycol/

water (1:1, v/v) bath. The temperature was controlled by a thermometer in the sample holder connected to the computer. In all cases the anisotropy was measured between 10 and 75 °C by taking steps of 5 °C and allowing the solutions to equilibrate for 15 min.

Preparation of *Cast* Bilayers for XRD. Acidic aqueous dispersions of amphiphilic dendrimers were prepared by the methanol injection method. Special Si single-crystal wafers, cut along the (501) plane, were used for low-angle measurements. Aliquots of the colloidal dispersions (2 mL) were left to dry on these Si wafers in a desiccator over sodium hydroxide. The specimen chamber was maintained at 20 °C and flushed with air of 20% relative humidity during the XRD measurements. The patterns were digitally recorded. Peak positions were obtained using peak-fitting JANDEL software.

Osmotic Experiments. A stock solution of **A5** in water was prepared by injecting 7.612 mg of **A5** dissolved in 100 μL of methanol/THF (1:2 v/v) into a 0.50 M sucrose solution (pH = 1, preheated at 60 °C, 5 mL) with stirring. Small aliquots (100 μL) of this stock solution were added to 2.5 mL of solutions containing 0.03−0.80 M sucrose. After the solution was mixed for 10 min, the absorption was measured at 450 nm.

Langmuir−Blodgett Experiments. Monolayer experiments were performed on a thermostated, home-built trough at 20 °C. The surface pressure was measured using the Wilhelmy plate method. Plates made of platinum or filter paper gave identical results. On the water subphase (pH = 7), 50 μL of a solution of the amphiphiles in $CHCl_3$ was spread and allowed to evaporate. To establish the stability of the monolayer, the surface pressure was maintained at a constant value of 10 mN/m. The monolayer area was found to remain constant for more than 8 h, indicating that the monolayers are stable. The rate of compression was 50 mm^2/s. Deposition experiments were performed at a constant surface pressure of 25 mN. A glass slide of 7.4 cm × 1.5 cm was dipped 20 mm into the subphase at a constant speed of 4 mm^2/s. Brewster angle microscope experiments were carried out with an NFT BAM1 instrument, manufactured by Nano Film Technology, Goettingen. The instrument was equipped with a 10 mV He−Ne laser with a beam diameter of 0.68 mm operating at 632.8 nm. Reflections were detected using a CCD camera.

Acknowledgment. We thank D. Hubert (Laboratory of Polymer Chemistry, Eindhoven University of Technology) for assistance with dynamic light-scattering measurements and B. de Waal (Laboratory of Organic Chemistry, Eindhoven University of Technology) for the synthesis of the palmitoyl-modified dendrimers. A. Roelofsen, H. Geurts (Department of Organic Chemistry, University of Nijmegen), E. Currie (Department of Physical and Colloidal Chemistry, University of Wageningen), Prof. Dr. A. J. Schouten, and P. J. Werkman (Department of Polymer Chemistry, University of Groningen) are acknowledged for their help with monolayer experiments. Special thanks are extended to Prof. Dr. P. M. Frederick and P.H.H. Bomans (Department of Pathology, University of Limburg, Maastricht) for the cryoelectron microscopy measurements and discussions. The Dutch Foundation for Chemical Research (SON) and DSM Research are acknowledged for an unrestricted research grant.

JA9736774